# Communications to the Editor

## Influence of Tensile Stress on the Molecular Mobility in Polycarbonate Visualized by Localized $^1$H NMR Spectroscopy

**F. Weigand and H. W. Spiess***

*Max-Planck-Institut für Polymerforschung, Postfach 3148, D-55021 Mainz, Germany*

*Received May 23, 1995*

*Revised Manuscript Received June 20, 1995*

**Introduction.** Molecular mobility is an important factor determining the macroscopic properties of polymeric materials.[1] Spatial variations of molecular parameters, depending on the processing conditions or the treatment of the polymeric material, lead to nonuniform and spatially dependent macroscopic behavior. For a systematic improvement of the manufacturing processes and the characterization of polymers, methods are needed which record the spatial dependence of molecular parameters like molecular motion. Solid-state NMR is particularly suited for this purpose, because it has provided a wealth of information about the time scale and the geometry of rotational motions in polymers.[2] Moreover, it can be combined with imaging techniques to provide spatial information.[3] On a phantom of polycarbonate and low-density polyethylene we have recently shown that solid-state $^1$H NMR wide-line spectroscopy in combination with magnetic field gradients for spatial encoding can indeed provide spatially resolved dynamical information for rigid bulk samples.[4] It is the purpose of this paper to demonstrate that localized $^1$H NMR spectroscopy can be employed for visualizing the immobilization of the molecular mobility in polymer materials from industrial laboratories.

A cold-drawn specimen of Bisphenol A polycarbonate (PC), kindly provided by BAYER AG, Leverkusen, was used in the investigation. The molecular dynamics of PC have been the subject of numerous studies. Solid-state $^1$H, $^2$H, and $^{13}$C NMR have established that besides methyl group rotation in the isopropyl group the prominent molecular dynamics involves 180° flips of the phenylene moieties.[5-8] Moreover, the relation of this process with the mechanically active low temperature $\gamma$-relaxation of PC was elucidated by 2D-exchange spectroscopy[2] of PC samples under tensile stress.[9,10] Likewise, partial immobilization of the phenylene mobility on cold drawing was detected.[10] In this experiment $^2$H NMR demonstrated that drawing to $\gamma = 1.7$ resulted in a 10 K temperature shift of the $T_1$ relaxation time curve with respect to the undrawn sample. Furthermore, the fraction of the slow component in the decay was enhanced, also showing a 10 K shift. Both effects indicated a decrease in phenylene mobility caused by the cold drawing. Alternatively, application of high hydrostatic pressure leads to the same behavior.[11] The drawing hardly changes the density of the sample at all,[10] vide infra.

* To whom correspondence should be addressed.

Cold drawing of PC causes necking of the macroscopic sample in height and width as shown schematically in Figure 1. It also leads to partial chain alignment, which can be seen in a polarizing microscope. Our sample (Makrolon M2800) was cold drawn at room temperature to a maximum elongation $\gamma = 1.7$ in the necking region. Under these drawing conditions crazes are not occurring, however, a small fraction of shear bands cannotbe avoided. The yield point occurred at a stress of approximately 59 MPa. Figure 1 also displays a picture of this sample under the polarizing microscope with crossed polarizers. In the unstressed area (left) light is transmitted through the specimen (bright areas). The white area is surrounded by colored shadows attributed to the pressure necessary to fix the sample in the drawing device. Adjacent to this region, there is the transition to the necking part (neck indicated by an arrow) with only weak white transmission at the borders before the sample ends with the region of cold flow where no polarized light is transmitted. The weak white transmissions at the borders disappear by rotating the sample under the polarized light, indicating that the alignment due to the stress is not uniaxial in the neck area. With localized NMR spectroscopy one can now check whether the molecular dynamics of the polymer indeed changes in the necking region. Since the material is mostly affected in the drawing direction, it is sufficient to encode the space via a magnetic field gradient in the drawing direction only (one-dimensional image).

For simplicity, $^1$H NMR is used. In principle, one could record $^1$H wide-line spectra.[4] However, as noted above, the immobilization effect due to drawing is rather small. Thus, more sophisticated methods are needed to detect such subtle changes. The pulse sequence should be simple and sensitive to different mobility changes. Among the different multiple-pulse sequences[12] the simplest (OW-4)[13,14] was found particularly suited to the employment of line narrowing which partially reduces the dipolar coupling between the protons. With the OW-4 sequence multiple solid echoes are generated and the dipole–dipole coupling appears inactive under stroboscopic observation of the echo maxima. Because of this averaging effect, the sequence is used in solids such that only an effective transverse relaxation process with a relaxation time $T_{2\mathrm{eff}}$ remains. The corresponding relaxation rate, $T_{2\mathrm{eff}}^{-1}$, which depends on the molecular dynamics in the sample, is most sensitive to slow thermal motions up to about $10^4$ Hz. This was checked by applying the OW-4 sequence to different polymers including polycarbonate, poly(ethylene oxide), and poly(methyl methacrylate).

**NMR Experiments.** To detect the $T_{2\mathrm{eff}}$ decay as a function of a spatial coordinate, a two-dimensional NMR experiment[2] is necessary. Therefore, the OW-4 sequence was combined with a spatial encoding sequence. Due to the large $^1$H line width of glassy polymers, standard imaging techniques cannot be applied. Thus, a special sequence[15] based on magic sandwich echoes (MSE) was used which is very robust in delivering

0024-9297/95/2228-6361$09.00/0 

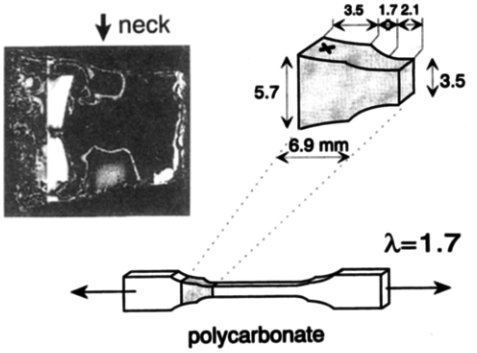


**Figure 1.** Geometry of the polycarbonate sample with a pictureof the stress transitional area under the polarizing microscope. The sample exhibits the transition to a necking region from drawing. Picture: In the region of cold flow (right) nearly no polarized light is transmitted through the sample because of the high orientation due to the drawing.

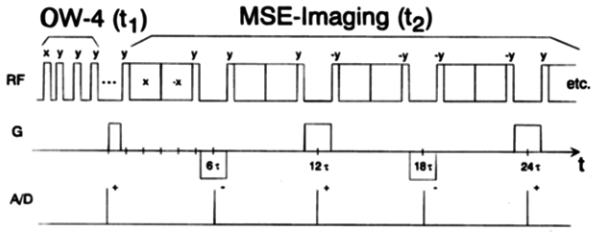


**Figure 2.** Two-dimensional pulse sequence for localized $T_{2eff}$ detection. Data sampling takes place stroboscopically every $6\tau$, i.e., the cycle time. All radio-frequency (rf) pulses with given phases are 90° pulses. During the sandwiches of the MSE sequence, $x$ and $-x$ denote the phases of permanent rf irradiation for the duration of $2\tau$. The field gradient $G$ is used only in the absence of rf irradiation. It is inverted in successive windows to account for a change in sign of the magic echo of every $6\tau$. In a Fourier imaging scheme a two-dimensional data set is recorded by stepping the number of solid echoes in the OW-4 sequence successively.

sufficient spatial resolution in solids.[4] The full 2D pulse sequence is given in Figure 2. The data are sampled in the $t_2$ dimension stroboscopically every $6\tau$, while their amplitude is encoded by the number of solid echoes applied in the $t_1$ dimension. This number of solid echoes is incremented successively in the 2D experiment from 1 to 32. Thus, the information about the molecular mobility is spatially encoded for a given portion of the PC sample, thereby allowing direct correlation of microscopic spectral and macroscopic spatial information.

The NMR experiments were performed at room temperature on a Bruker MSL-300 spectrometer ($^1$H resonance frequency 300.23 MHz) in combination with a commercial probehead that has been modified by a home-built gradient system. The gradient strength applied in the $B_1$ direction was 90 mT/m, with a switching time less than 900 ns. The 90° pulse length was 2 $\mu$s, with an echo time (period between the 90° pulses of the OW-4 sequence) in the $t_1$ dimension of 18 $\mu$s. For recording the spatial projections in the $t_2$ dimension the cycle time was $6\tau = 60$ $\mu$s, and 32 scans were coadded for each $t_1$ increment. Thus, with a repetition time of 3 s it took only 52 min to acquire the whole 2D data set. The sample was positioned such that the static magnetic field $\vec{B}_0$ was perpendicular to the draw direction. It was checked in previous experiments that the radio-frequency (rf) is sufficiently homogeneous over the sample length. For data analysis only the spatial dimension ($t_2$) is Fourier transformed and the $t_1$ dimension is left in the time domain. These time data display the $T_{2eff}$ decay for each spatial position of the sample.

**Results and Discussion.** Figure 3 shows the results of the experiment applied to polycarbonate. The following different effects are observed:

On the left a typical $T_{2eff}$ decay (triangles) normalized to 100% is presented for a fixed spatial position, indicated by the cross in Figure1. The decay can quantitatively be fitted (solid lines) with two superimposed exponential decays, a fast component (squares) and a slow component (circles). In order to check the nature of the two components different experiments, not presented here,[16] were performed. There, CP MAS on $^{13}$C nuclei was used with different delay times before the CP.[2] These experiments showed that the short time behavior of the $T_{2eff}$ results predominantly from the phenylene $^1$H, whereas the contribution of the methyl $^1$H is enhanced in the long time decay. However, both decays have contributions from both sites due to spin diffusion processes.

For every spatial position within the sample the relaxation data can be fitted with such a biexponential decay and the resulting parameters are presented on the right in Figure 3. In these plots the fitted values of the relaxation rate $T_{2eff}^{-1}$ (inverse of the $T_{2eff}$ relaxation time) are shown over the spatial coordinate of the sample. The average error of the fitted values is approximately 15%. For a better spatial assignment the spin-density projection in arbitrary units is also plotted (broken lines). Both pictures provide $T_{2eff}^{-1}$ contrast between the unstressed material and the region of cold flow (right part of the sample) as noted in ref 17 already. While the spin-density contrast merely reflects the change in the dimensions of the rod (the slightly higher material density in the drawn region is negligible), the relaxation rate characterizes the molecular mobility. In the region of cold flow $T_{2eff}^{-1}$ is higher than that in the unaffected material, indicating reduced mobility.

A comparison of the two mobility pictures shows a larger contrast in the short time behavior. There, we also find much higher values of $T_{2eff}^{-1}$ between 8 and $20 \times 10^3$ s$^{-1}$ representing faster magnetization coherence decay due to a higher rigidity. The larger contrast shows that drawing mainly affects the short time behavior of the relaxation which is phenylene enhanced. Fast motional sections such as methyl group rotations with small relaxation rates $T_{2eff}^{-1}$ are more resistant to drawing, which is reflected in the shape of the immobilization curve shown in the upper plot. Indeed, in separate experiments the $T_{2eff}^{-1}$ rates at room temperature were determined as $8.7 \times 10^3$ s$^{-1}$ (short time) and $2.6 \times 10^3$ s$^{-1}$ (long time) of virgin and $19.9 \times 10^3$ s$^{-1}$ (short time) and $3.9 \times 10^3$ s$^{-1}$ (long time) of cold-drawn PC, respectively[16] (experimental error ca. 10%), in remarkable agreement with the spatially dependent measurements (cf. arrows in Figure 3).

The spatial distribution of $T_{2eff}^{-1}$ correlates well with the stress information contained in the photograph in Figure 2. Just before the neck the drawing starts to affect the PC sample. Behind the neck, the region of maximum cold flow occurs and nearly no light is transmitted through the sample because of the high orientation due to the drawing. In this region we also find the maximum values for the relaxation rate $T_{2eff}^{-1}$. Moreover, it should be noted that the maximum of the immobilization occurs spatially displayed by ca. 1 mm toward the drawn region, if compared with the spin density and the photograph, just beyond the spatial

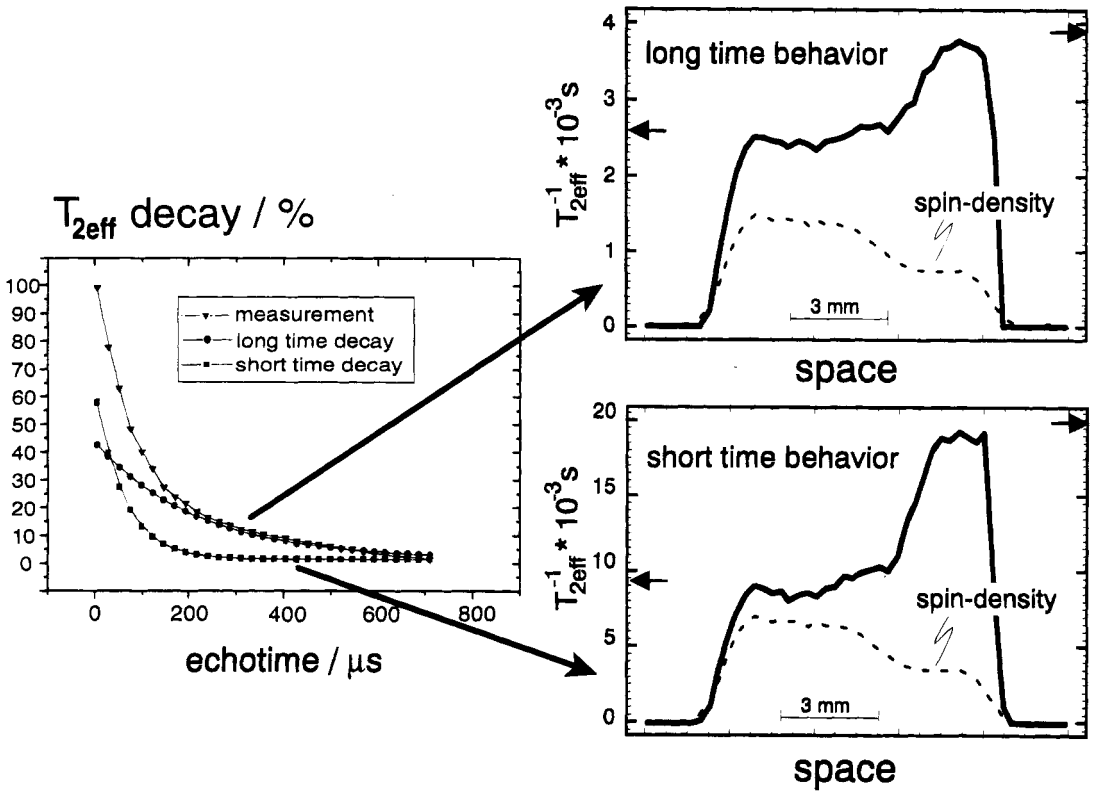


**Figure 3.** Left: Typical $T_{2eff}$ decay (triangles) normalized to 100% for a fixed spatial position, indicated by the cross in Figure 1. The decay consiss of two components, a fast (circles) and a slow (squares) exponential, which were fitted to the curve. Right: Fitted values of the relaxation rate $T_{2eff}^{-1}$ (inverse of the $T_{2eff}$ relaxation time) over the space. For a better spatial assignment the spin-density projection is drawn as a broken line in arbitrary units. Both pictures provide $T_{2eff}^{-1}$ contrast between the unstressed material and the region of cold flow (right part of the sample). The relaxation rate characterizes the molecular mobility indicating the immobilization effect in polycarbonate due to the drawing.

resolution of 0.7 mm in our experiment.

In order to reconcile the changes in mobility determined here via $T_{2eff}^{-1}$, this parameter was measured in virgin PC as a function of temperature between 188 and 428 K to find the temperature shift corresponding to the mobility change resulting from the drawing. Both, short time and long time behavior, show decreasing $T_{2eff}^{-1}$ values with increasing temperature proportional to $1/T$ in an Arrhenius plot. The changes in the relaxation rate $T_{2e}^{-1}$ due to the drawing (cf. Figure 3) would correspond to a temperature shift $\Delta T_{\text{short time}} \approx 85 \pm 25$ K.

Since different dynamic processes are discussed for PC, the question arises as to whether this temperature shift belongs to large amplitude motions (phenyl flips)[5-8] or small-angle motions[6] and main-chain wiggling.[18] It is known from $T_1$ measurements and 2D NMR[10] which probe molecular motions around $10^8$ and 10 Hz, respectively, that the slowing down of the phenyl flip rate due to drawing to $\gamma = 1.7$ corresponds to a temperature shift of $\Delta T \approx 10$ K only. This nicely correlates with the change in the overall density, which is changing from $\varrho = 1.19802$ g/cm$^3$ in the virgin to $\varrho = 1.20143$ g/cm$^3$ in the drawn material. This difference likewise corresponds to a temperature shift of only $\Delta T_{\Delta\varrho} \approx 13 \pm 5$ K. In contrast, the density at a temperature decreased by 85 K would be $\varrho \approx 1.22$ g/cm$^3$ emphasizing that the effect of drawing on $T_{2eff}$ cannot be explained by changes in the macroscopic density of the sample. Thus, the changes in mobility resulting from drawing are not at all equivalent to a change in temperature: Changes of large-angle motions and the density would correspond to a temperature shift of 10–15 K and the motions detected by $T_{2eff}^{-1}$ to a shift of 85 K. Therefore, it is not surprising that the apparent temperature shift deduced from the long $T_{2eff}$ component (cf. Figure 3) is again different, $\Delta T_{\text{long time}} \approx 15$ K reflecting a mixture of both effects.

Most likely, $T_{2eff}^{-1}$ reflects small-amplitude motions as discussed, e.g., by Schaefer,[18] who determined main-chain wiggles with an amplitude of about 10°. Cold drawing affects the distribution of the free volume, leads to a partial orientation of the polymer chain, and apparently causes substantial changes of this restricted mobility. Thus, the drawing mainly influences the intermolecular interactions, resulting in a change of the packing.

Although the spatial resolution of our localized NMR experiment (about 0.7 mm) is rather poor compared to other image-forming methods like electron microscopy, we have demonstrated here the unique advantage of spatially resolved NMR: It allows the correlation of parameters sensitive to molecular dynamics with macroscopic space, as demonstrated in the study of elastomers, where the mobility is so high that liquid-type imaging methods can be employed.[3] To our knowledge, our study presents the first example that subtle immobilization effects resulting from processing are detected with spatial resolution in a glassy polymer. Because many materials are transparent to radio-frequency waves, this type of investigation can also be applied to many optically nontransparent objects.

**Acknowledgment.** The authors thank Dr. R. Plaetschke, BAYER AG, Leverkusen, for providing the polycarbonate sample, Dr. R. H. Lewis for his help with the CP MAS measurements, and Prof. Dr. B. Blümich and Dr. J. Lehmann, Röhm AG, for stimulating discus-

sions. Drawn PC was made available by Dr. T. Pakula. F. W. acknowledges a stipend of the "Studienstiftung des deutschen Volkes". We also thank "Dr. Otto Röhm Gedächtnisstiftung, Darmstadt" for a donation.

## References and Notes

(1) *Principles of Polymer Engineering;* McCrum, N. G., Buckley, C. P., Bucknall, C. B., Eds.; Oxford University Press: Oxford, U. K., 1988.
(2) *Multidimensional Solid-State NMR and Polymers;* Schmidt-Rohr, K., Spiess, H. W., Eds.; Academic Press: London, U. K., 1994.
(3) *Magnetic Resonance Microscopy: Methods and Applications in Materials Science, Agriculture, Biodmedicine;* Blümich, B., Kuhn, W., Eds.; VCH: Weinheim, Germany, 1992.
(4) Weigand, F.; Demco, D. E.; Blümich, B.; Spiess, H. W., accepted for publication in *Solid State Nucl. Magn. Reson.*
(5) Inglefield, P. T.; Jones, A. A.; Lubianez, R. P.; O'Gara, J. F. *Macromolecules* **1981**, *14*, 288.
(6) Spiess, H. W. *Colloid Polym. Sci.* **1983**, *261*, 193.
(7) Inglefield, P. T.; Amici, R. M.; O'Gara, J. F.; Hung, C.-C.; Jones, A. A. *Macromolecules* **1983**, *16*, 1552.
(8) Schaefer, J.; Stejskal, E. O.; McKay, R. A.; Dixon, W. T. *Macromolecules* **1984**, *17*, 1479.
(9) Hansen, M.; Blümich, B.; Boeffel, S.; Spiess, H. W.; Morbitzer, L.; Zembrod, A. *Macromolecules* **1992**, *25*, 5542.
(10) Hansen, M.; Boeffel, S.; Spiess, H. W. *Colloid Polym. Sci.* **1993**, *271*, 446.
(11) Hansen, M.; Kulik, A.; Prins, K., Spiess, H. W. *Polymer* **1992**, *30*, 2231.
(12) *High Resolution NMR in Solids;* Mehring, M., Ed.; Springer: London 1983.
(13) Ostroff, E. D.; Waugh, J. S. *Phys. Rev. Lett.* **1966**, *16*, 1097.
(14) Mansfield, P.; Ware, D. *Phys. Rev.* **1968**, *168*, 318.
(15) Weigand, F.; Blümich, B.; Spiess, H. W. *Solid State Nucl. Magn. Reson.* **1994**, *3*, 59.
(16) Weigand, F. Ph.D. Thesis, University of Mainz, Mainz, Germany, 1995.
(17) Blümich, B.; Blümler, P.; Fülber, C.; Scheler, U.; Weigand, F. *Makromol. Symp.* **1994**, *87*, 187.
(18) Schaefer, J.; Stejskal, E. O.; Perchak, D.; Skolnick, J.; Yaris, R. *Macromolecules* **1985**, *18*, 368.

MA950394S